Available online at www.sciencedirect.com
SCIENCE DIRECT®
Journal of Magnetic Resonance 164 (2003) 182–186
JMR Journal of Magnetic Resonance
www.elsevier.com/locate/jmr

Communication

A "Magic Sandwich" pulse sequence with reduced offset dependence for high-resolution separated local field spectroscopy

Alexander A. Nevzorov and Stanley J. Opella*

Department of Chemistry and Biochemistry, University of California, San Diego, La Jolla, CA 92093-0307, USA

Received 10 April 2003; revised 10 June 2003

Abstract

A pulse sequence for high resolution separated local field spectroscopy based on "magic sandwich" elements is demonstrated on a single crystal sample. Simulations and experimental results show that this pulse sequence has a reduced frequency offset dependence compared to PISEMA (polarization inversion spin exchange at the magic angle). As a result, it has a larger effective range of homonuclear decoupling, reduced zero-frequency spectral distortions, and more reliable scale factors for individual resonances. In addition, it is easier to setup on commercial spectrometers.

Keywords: Dipolar coupling; Sample alignment; PISEMA; Solid state NMR

The dipole–dipole interaction between two nuclei results in a local field that is a valuable source of information about molecular structure. When the coupling is between two covalently bonded nuclei in a rigid molecule the interpretation is particularly straightforward; since the internuclear distance is constant, the frequency splittings due to dipolar couplings yield very accurate measurements of the angles between the bonds and the direction of the applied magnetic field [1]. These angles provide input for structure determination as orientational restraints.

The local field that results from the dipole–dipole coupling between two different spin 1/2 nuclei is of particular interest for structure determination, especially those from ^{1}H–^{15}N amide sites in the backbone of a protein. Even in uniformly labeled proteins, the ^{15}N nuclei are "dilute" since there are relatively few nitrogens in proteins, they have a low gyromagnetic ratio, and nitrogens in peptide bonds are spaced evenly throughout the polypeptide backbone separated from each other by two intervening carbon atoms. By contrast, the ^{1}H nuclei are "abundant" since there are many of them and they are strongly coupled due to their high gyromagnetic ratio and density. The couplings among the remote ^{1}H spins complicate the heteronuclear dipolar coupling spectra of the ^{1}H–^{15}N pairs of interest for structure determination; this is the case whether the evolution of the heteronuclear dipolar coupling is monitored directly [2] or through spin-exchange between the heteronuclei. PISEMA (polarization inversion spin-exchange at the magic angle) [3] provides high-resolution heteronuclear dipolar coupling spectra, and can be used to obtain completely resolved spectra of uniformly ^{15}N-labeled proteins [4]. However, because it relies on off-resonance Lee–Goldburg [5] irradiation for homonuclear decoupling of the abundant ^{1}H spins, its performance is sensitive to the choice of ^{1}H carrier frequencies. In complex molecules, like proteins, there is a wide range of ^{1}H resonance frequencies due to their chemical shifts; in high magnetic fields this can be more than 10 kHz for an amide hydrogen, since its chemical shift tensor spans about 14 ppm [6,7], which makes it impossible to satisfy the necessary conditions for all sites simultaneously. This yields spectra where some resonances are narrower and more intense than others, and makes the experiment difficult to setup. In order to address these problems we have implemented the pulse sequence diagrammed in Fig. 1 that utilizes on-resonance pulses rather than frequency-switched

* Corresponding author. Fax: 1-858-822-4821.
E-mail address: sopella@ucsd.edu (S.J. Opella).

1090-7807/$ - see front matter © 2003 Elsevier Science (USA). All rights reserved.
doi:10.1016/S1090-7807(03)00240-4

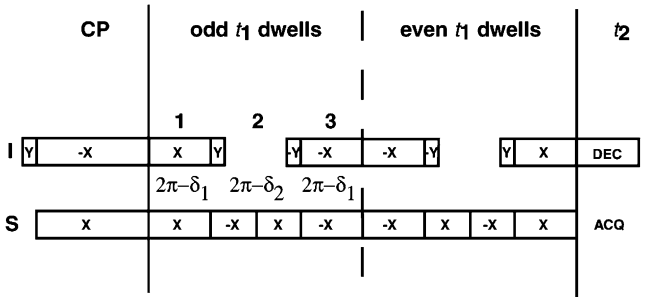

Fig. 1. Timing diagram for the double-resonance pulse sequence referred to as SAMMY. The heteronuclear interaction evolves during the first and third parts, and the homonuclear interaction vanishes over the cycle up to the third order in time. During the second part, the dilute spins (^{15}N) are decoupled from the abundant spins (^{1}H). Two $(\pi/2)_y$ pulses are inserted to achieve the transformation between the tilted and rotating frames. To achieve optimal decoupling, the contact times (parts 1 and 3) as well as the duration of the window (part 2) should be adjusted experimentally from their theoretical 2π values. In this work, $\delta_1 = 0$; $\delta_2 = 2\,\mu$s.

Lee–Goldburg irradiation to effect homonuclear ^{1}H decoupling. Its principal advantages compared to PISEMA are that it has a reduced offset dependence and it is easier to setup on commercial spectrometers.

Effective suppression of the heteronuclear couplings involving the remote spins is achieved during on-resonance Hartmann–Hahn cross-polarization (CP) transfer of magnetization. The heteronuclear dipolar interaction evolves under the flip-flop Hamiltonian [8], however, since the terms at different ^{1}H sites do not commute, they cause perturbations of the substantially larger local fields of interest. In order to obtain high-resolution heteronuclear dipolar spectra the homonuclear interactions among the various ^{1}H spins must be removed during the CP transfer. In PISEMA, this is accomplished by tilting the protons to the magic angle $\theta = 54.7°$ in the rotating frame by off-resonance Lee–Goldburg irradiation during the dipolar evolution time period [3]. Maladjustment of the offset frequencies due to the variation among ^{1}H chemical shifts has several undesirable effects. The theoretical scaling factor for the heteronuclear dipolar coupling, $\sin\theta = 0.82$, cannot be correct for all sites; and even small deviations from the magic angle can result in an appreciable residual homonuclear scaling factor, $(3\cos^2\theta - 1)/2$, which interferes with the removal of spin diffusion. By contrast, keeping the protons in either the X, Y plane or along the Z-axis minimizes the effect of the frequency spread due to the ^{1}H chemical shifts, since the derivative of $(3\cos^2\theta - 1)/2$ is zero at $\theta = 90°$ and $0°$. This is the basis for the design of the pulse sequence in Fig. 1, which we refer to as "SAMMY," since it incorporates "magic sandwiches" in the ^{1}H irradiation scheme to cancel the homonuclear terms in the average Hamiltonian. In essence, the fundamental building block of SAMMY represents a modification of the well-known "burst" or "magic sandwich" pulse sequence [9–13]. In this pulse sequence, it is implemented to accomplish the CP transfer between ^{15}N and ^{1}H while decoupling the protons from each other, rather than to obtain ^{1}H spin echoes or probe chemical shifts [9–12], therefore, the original order of applying the RF pulses in the magic sandwich has been changed. In SAMMY, the heteronuclear dipolar (t_1) evolution period is divided into three parts, each of which is equal to the duration of one 2π pulse. During the first and third parts, the system evolves under the many-body Hamiltonian that describes the interaction of a dilute S spin (e.g., ^{15}N or ^{13}C) with N abundant I spins (i.e., ^{1}H)

$$H_{1,3} = H_{\pm} - \frac{1}{2}H_{zz}. \tag{1}$$

The heteronuclear flip-flop and homonuclear dipolar Hamiltonians are given by

$$H_{\pm} = \sum_{i=1}^{N} \frac{a_i}{4}\left[S_{+}I_{-}^{(i)} + S_{-}I_{+}^{(i)}\right], \tag{2a}$$

$$H_{zz} = \sum_{i<j}^{N} b_{ij}\left[I_z^{(i)}I_z^{(j)} - \frac{1}{4}\left(I_{+}^{(i)}I_{-}^{(j)} + I_{-}^{(i)}I_{+}^{(j)}\right)\right], \tag{2b}$$

a_i and b_{ij} are the heteronuclear and homonuclear coupling constants, respectively. The Hamiltonian of Eq. (1) can be obtained by a 90°-y rotation to the tilted frame followed by the standard truncation of higher-order terms. During the second part, the S spins are decoupled from the I spins and the system evolves simply as

$$H_2 = H_{zz}. \tag{3}$$

Two intermediate $(\pm\pi/2)_y$ pulses are inserted to effect the necessary transformations between the tilted and rotating frames. The method of symmetrization of the cycle [13,14] yields cancellation of the homonuclear dipolar terms up to third-order in time. Using the results of Yoshida [15] for second-order symplectic integrators we obtain for the leading terms

$$\exp\left[\mathrm{i}t\left(H_{\pm} - \frac{1}{2}H_{zz}\right)\right]\exp(\mathrm{i}tH_{zz})\exp\left[\mathrm{i}t\left(H_{\pm} - \frac{1}{2}H_{zz}\right)\right] \approx \exp\left[2\mathrm{i}tH_{\pm} - \frac{\mathrm{i}t^3}{12}[H_{zz},[H_{zz},H_{\pm}]] + \mathrm{O}(t^4)\right]. \tag{4}$$

The cubic term in t presumably does not have an appreciable effect for the range of heteronuclear couplings studied (<10 kHz). Moreover, making the odd dwells a mirror image of the even dwells cancels the effects of ^{1}H chemical shift evolution over two dwell intervals. The system evolves effectively as $2H_{\pm}$ over the entire cycle and the dwell time is approximately equal to the length of a 4π pulse. The lengths of the first and third parts, as well as the interval between the two $(\pm\pi/2)_y$ pulses are varied slightly as part of the experimental tune-up procedure. It has been found semi-empirically that optimal performance is achieved when the time between the two

$(\pm\pi/2)_y$ pulses is about 2 μs shorter than the 2π time. This may be due to inaccuracies in the determination of the RF field strength or the finite length of the pulses during which some homonuclear dipolar evolution occurs. In addition, it has been found from numerical simulations that the alternation of the phases of the π-pulses during the middle interval provides more effective heteronuclear decoupling.

The experimental implementation of the pulse sequence shown in Fig. 1, and its comparison to PISEMA was performed on a single crystal of [^{15}N]acetyl-leucine at an arbitrary orientation in a homebuilt double-resonance probe with a 5 mm-inner diameter solenoid coil. The rest of the spectrometer consisted of a Bruker (Billerica, MA) Avance console equipped with high-power amplifiers interfaced with a Magnex (Oxford, UK) 750/54 magnet. The two-dimensional spectrum shown in Fig. 2 was obtained with the pulse sequence diagrammed in Fig. 1 at a ^{1}H resonance frequency of 750 MHz, which is high enough to result in a significant frequency spread among the ^{1}H chemical shifts. The length of a $\pi/2$ pulse was carefully measured at 4.15 ± 0.05 μs. Although each molecule has only one ^{1}H–^{15}N bond, the spectrum has four dipolar splittings because there are four unique sites in the unit cell of the crystal.

Theoretical simulations were performed on an eight-spin system where the ^{1}H bath consisted of $N = 7$ protons using Matlab (Mathworks). The atomic coordinates were taken from a α-helix tilted approximately 30° away from parallel to the direction of the magnetic field. Protons within a 3.3 Å radius sphere centered at

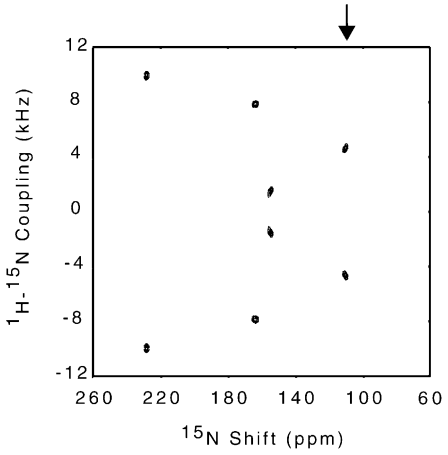

Fig. 2. Experimental two-dimensional ^{1}H–^{15}N heteronuclear dipolar coupling/^{15}N chemical shift spectrum of a single crystal of *N*-acetyl-leucine at an arbitrary alignment relative to the direction of the applied magnetic field. The spectrum was obtained at a ^{1}H resonance frequency of 750 MHz using the pulse sequence diagrammed in Fig. 1. The $\pi/2$ pulse was calibrated at 4.15 μs and the optimal time between the $(\pm\pi/2)_y$ pulses was found to be 14.6 μs. Peak 4 is marked with the arrow.

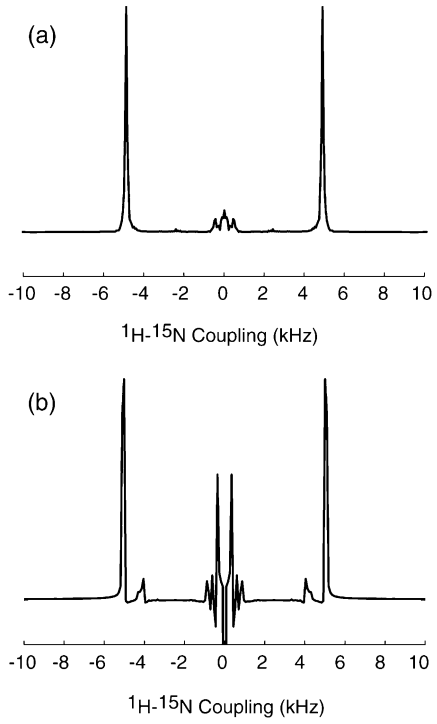

Fig. 3. Simulations of one-dimensional heteronuclear dipolar coupling spectra with the ^{1}H carrier frequency on-resonance: (a) SAMMY; (b) PISEMA.

^{15}N are included in the simulations. This reproduces the dissipating effect of the bath fairly well, and increasing N to 10 ($r = 3.95$ Å) did not have a significant effect on the overall appearance of the spectra, but did substantially increase the amount of time needed for the calculations. Fig. 3 compares simulated one-dimensional heteronuclear dipolar coupling spectra from SAMMY (Fig. 3a) and PISEMA (Fig. 3b) experiments. In the simulations, the directly bonded ^{1}H was on-resonance, and the other six protons were assigned random chemical shifts distributed within ±5 ppm. A notable difference is a decreased zero-frequency distortion of the spectrum in Fig. 3a, which reflects the evolution of the heteronuclear

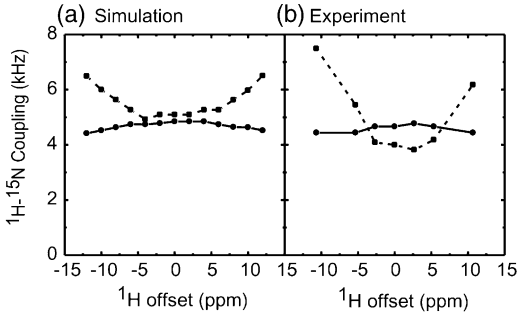

Fig. 4. Simulations (a) and experimental measurements (b) of the magnitude of the dipolar coupling as a function of offset of the ^{1}H resonance frequency. Continuous line is SAMMY. Dashed line is PISEMA.

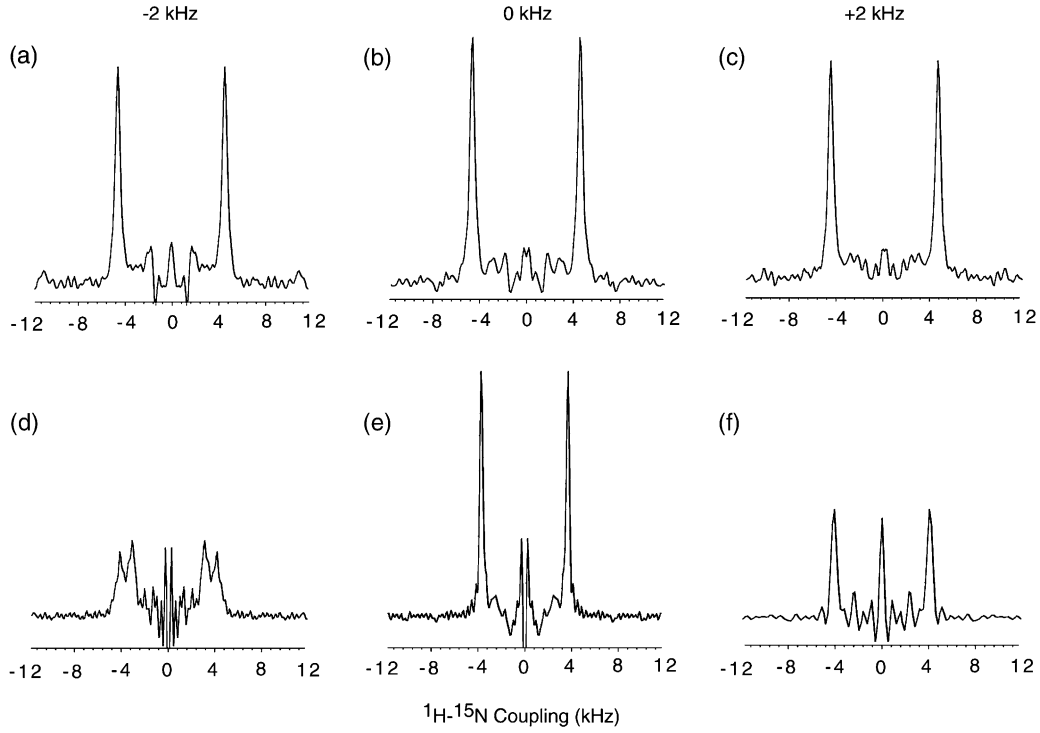

Fig. 5. Experimental heteronuclear dipolar coupling spectra extracted as one-dimensional slices from two-dimensional spectra for peak 4 marked with an arrow in Fig. 2: (a)–(c) were obtained with SAMMY; (d)–(f) were obtained with PISEMA. (a) and (d) correspond to −2 kHz ^{1}H resonance offset; (b) and (e) correspond to on-resonance; (c) and (f) correspond to +2 kHz ^{1}H resonance offset.

couplings in the X, Y plane. Tilting the ^{1}H spins to the magic angle causes some additional low-frequency nutation in the PISEMA spectra.

Simulations of the dependence of the measured heteronuclear couplings on the ^{1}H carrier offsets are compared in Fig. 4a, and the corresponding experimental dependencies are compared in Fig. 4b. The offset dependence of the scaling factor is significantly less for SAMMY than for PISEMA in both the simulated and experimental comparisons.

One-dimensional spectral slices through the resonance marked with an arrow in Fig. 2 are shown in Fig. 5 for spectra obtained with three different ^{1}H carrier frequencies. PISEMA yields the narrowest linewidths under optimal on-resonance conditions. However, with the ^{1}H carrier 2 kHz off-resonance in either direction, the spectra obtained with SAMMY are significantly better than that obtained with PISEMA. We note that the splitting in Fig. 5b is noticeably larger than that in Fig. 5e, possibly because the proton bath may have different chemical shifts than the directly bonded proton. Therefore, the proton frequency for optimal homonuclear decoupling may not coincide with the resonant frequency for the covalently bonded proton, and this leads to the slightly different scaling factor for the heteronuclear coupling, $\sin\theta$, as shown in Fig. 3. By contrast, the scaling observed in the SAMMY spectra remains nearly constant for all three frequencies, since the derivative of $\sin\theta$ is zero at $\theta = 90°$, which renders the scaling less sensitive to the frequency offset.

Both the simulated and experimental data shown in the figures demonstrate that heteronuclear dipolar spectra obtained with SAMMY are less sensitive to ^{1}H frequency offset than those obtained with PISEMA. This is advantageous in NMR studies of complex molecules at high fields where there is a significant range of ^{1}H chemical shifts. SAMMY has the additional advantage of being easier to setup, since only a single pulse width needs to be measured and there are no frequency offsets to be calibrated. SAMMY expands the capability for high-resolution solid-state NMR of proteins by reducing the offset dependence of the ^{1}H carrier frequency.

Acknowledgments

We thank C.H. Wu for building the probe used in these experiments, A. Mrse for assistance with the instrumentation and spectroscopy, D. Jones and J.S. Struppe for helpful discussions, and D. Thiriot and A. DeAngelis for testing the pulse sequence on protein samples. This research was supported by Grants R37GM24266, RO1GM29754, PO1GM64676, and P41EB002031 from the National Institutes of Health.

References

[1] G.E. Pake, Nuclear resonance absorption in hydrated crystals: fine structure of the proton line, J. Chem. Phys. 16 (1948) 327.

[2] R.K. Hester, J.L. Ackerman, B.L. Neff, J.S. Waugh, Separated local field spectra in NMR: determination of structure of solids, Phys. Rev. Lett. 36 (1976) 1081–1083.

[3] C.H. Wu, A. Ramamoorthy, S.J. Opella, High-resolution heteronuclear dipolar solid-state NMR spectroscopy, J. Magn. Reson. A 109 (1994) 270–272.

[4] F.M. Marassi, A. Ramamoorthy, S.J. Opella, Complete resolution of the solid-state NMR spectrum of a uniformly ^{15}N-labeled membrane protein in phospholipid bilayers, Proc. Natl. Acad. Sci. USA 94 (1997) 8551–8556.

[5] W.I. Goldburg, M. Lee, Nuclear magnetic resonance line narrowing by a rotating rf field, Phys. Rev. Lett. 11 (1963) 255–258.

[6] R. Gerald, T. Bernhard, U. Haeberlen, J. Rendell, S.J. Opella, Chemical shift and electric field gradient tensors for the amide and carboxyl hydrogens in the model peptide *N*-acetyl-D,L-valine. Single-crystal deuterium NMR study, J. Am. Chem. Soc. 115 (1993) 777–782.

[7] C.H. Wu, A. Ramamoorthy, L.M. Gierasch, S.J. Opella, Simultaneous characterization of the amide ^{1}H chemical shift, ^{1}H–^{15}N dipolar, and ^{15}N chemical shift interaction tensors in a peptide bond by three-dimensional solid-state NMR spectroscopy, J. Am. Chem. Soc. 117 (1995) 6148–6149.

[8] Z. Gan, Spin dynamics of polarization inversion spin exchange at the magic angle in multiple spin systems, J. Magn. Reson. 143 (2000) 136–143.

[9] W.-K. Rhim, A. Pines, J.S. Waugh, Violation of the spin-temperature hypothesis, Phys. Rev. Lett. 25 (1970) 218–220.

[10] W.-K. Rhim, A. Pines, J.S. Waugh, Time-reversal experiments in dipolar-coupled spin systems, Phys. Rev. B 3 (1971) 684–696.

[11] K. Takegoshi, C.A. McDowell, A "magic-echo" pulse sequence for the high-resolution NMR spectra of abundant spins in solids, Chem. Phys. Lett. 116 (1985) 100–104.

[12] A. Pines, W.-K. Rhim, J.S. Waugh, Homogeneous and inhomogeneous nuclear spin echoes in solids, J. Magn. Reson. 6 (1972) 457–465.

[13] M. Hohwy, N.C. Nielsen, Elimination of high order terms in multiple pulse nuclear magnetic resonance spectroscopy: application to homonuclear decoupling in solids, J. Chem. Phys. 106 (1997) 7571–7586.

[14] D.P. Burum, W.-K. Rhim, Analysis of multiple pulse NMR in solids. III, J. Chem. Phys. 71 (1979) 944–956.

[15] H. Yoshida, Construction of higher-order symplectic integrators, Phys. Lett. A 150 (1990) 262–268.